Structural Design for On-Line Process Optimization: II. Application to a Simulated FCC

C. Loeblein and J. D. Perkins
Centre for Process Systems Engineering, Imperial College, London SW7 2BY, United Kingdom

A previously proposed methodology for analyzing the economic performance of different structures of an integrated model predictive regulatory control and on-line optimization system is illustrated using the simulated case study of a fluid-catalytic cracker. The economic performance of two previously proposed regulatory control structures, the conventional and riser-regenerator control structures, is assessed both in isolation and as part of a real-time optimization system. The results show that the economic performance of the conventional structure is superior when operated in isolation. The theory, however, predicts that an optimally configured real-time optimization system based on the riser-regenerator structure will deliver superior performance overall. The predictions of the method were confirmed using Monte Carlo simulations.

Introduction

With the application of steady-state on-line optimization techniques, considerable economic benefits in process operations can be achieved (Cutler and Perry, 1983). In order to maintain the economically optimal operation of the process in the presence of slow disturbances and uncertainties, process measurements are taken and used to update a set of model parameters in an estimation step. The optimization model is then optimized with the estimated parameters and a new optimal steady-state operating point is determined. An important prerequisite for a successful implementation of on-line optimization techniques is that a well-tuned regulatory control system is in place. The regulatory control system brings the process to the new optimal steady state determined by the optimizer and holds the process as close as possible to this operating point until a future point in time when another on-line optimization cycle starts. Nowadays, this is often achieved using model predictive control (MPC) techniques (Qin and Badgwell, 1996). Constraints on the manipulated and controlled variables of the process can be incorporated at this level in order to operate the process closer to economically important constraints, prevent manipulated variables from saturation, and take immediate action in the case of signal or valve failures.

In the first part of this article, a methodology estimating the dynamic economic performance of a model predictive regulatory control (MPC) system in terms of regulatory constraint backoff from process constraints has been presented. The resulting method has been integrated with the established method of the average deviation from optimum analyzing the likely economic benefit of implementing an on-line optimizer on a plant (de Hennin et al., 1994; Loeblein and Perkins, 1996). Thus, the economic performance of different structures of the integrated system for on-line optimization and regulatory control of the process can be estimated and important structural design decisions for the on-line optimization or regulatory control system such as the selection of regulatory control set points, estimated parameters, process measurements, or choice of the optimization model can be taken with regard to the performance of the overall system. In this article, the theory is illustrated using the simulated case study of a fluid-catalytic cracker (FCC).

The FCC process is described together with the model representing the process. The dynamic economics of two different regulatory control structures are analyzed. The effect of the dynamic economics of the regulatory control layer and its structure on the performance of the on-line optimization system are illustrated, followed by some conclusions.

Modeling and Optimization of a FCC

The method of the average deviation from optimum for the analysis of the economic performance of the integrated MPC regulatory control and on-line optimization system is

Correspondence concerning this article should be addressed to J. D. Perkins.

demonstrated on a case study which consists of the optimization and control of a FCC. For a given set of uncertain parameters and fast disturbances, different structures of the on-line optimization and regulatory control system are compared and the structure with the best economic performance is determined. In the next sections, a short introduction to the FCC process is given together with an overview on relevant literature of modeling, control and optimization of FCC units. After that, the results of the method of the average deviation from optimum are presented.

Introduction to the FCC process

FCC is one of the most important processes in the petrochemical industry. It is operated to convert heavy, high boiling hydrocarbon petroleum fractions into lighter and more valuable components such as gasoline, light olefins (C_3s and C_4s), and light gases. Due to its large throughput and the high product-feed upgrade, the economically optimal operation of a FCC is important for the overall profit of a refinery. The FCC process is, therefore, subject to the application of advanced control and optimization algorithms in order to improve its economic performance (McFarlane et al., 1993).

The flowsheet of a FCC process is shown in Figure 1. Heavy gas oil from other refinery units is preheated and mixed with hot catalyst from the regenerator. The cracking reactions occur while the mixture of vaporized oil and catalyst flows up to the riser. The heat of the regenerated catalyst provides the necessary heat of vaporization and heat of reaction for the endothermic cracking reactions. Having reached the separator, which is sometimes also referred to as the reactor, the vaporized products and the spent catalyst are separated. The products are removed overhead while the catalyst is returned to the stripping section of the separator where steam is injected to remove volatile hydrocarbons from the catalyst. As a byproduct of the cracking reactions, coke is formed, which is deposited on the catalyst and reduces its activity. Due to the reduced activity of the catalyst, continuous regeneration is necessary. The spent catalyst is transported to the regenerator where it is fluidized by air. Due to the presence of hot air, the carbon deposited on the catalyst is burned off by reacting with the oxygen in the air, which also heats up the regenerated catalyst. The flue gas travels up the regenerator into the cyclones where entrained catalyst is removed and returned to the bed.

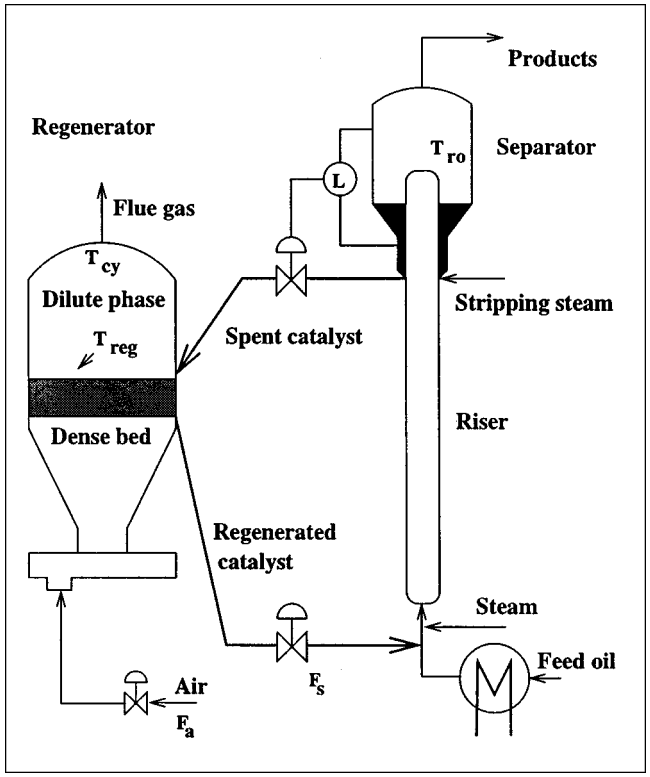

Figure 1. FCC plant.

FCC model

Several authors have made substantial efforts to model the behavior of FCC units. A detailed review of recent work on FCC modeling can be found in the article by Arbel et al. (1995). Contributions to the modeling of FCC units vary from regenerator models (Errazu et al., 1979) over kinetic models for the reactions taking place in the reactor riser, such as the four-lump model of Lee et al. (1989) and the ten-lump model of Jacob et al. (1976), to models describing the entire process, where the most commonly used are the ones by McFarlane et al. (1993), Lee and Groves (1985) and Arbel et al. (1995).

The model used for this case study is the one developed by Lee and Groves (1985) with slight modifications according to Hovd and Skogestad (1993). It is based on the three-lump reactor model which comprises the main components in a FCC unit. The chemical species are lumped into the three pseudo-components gas oil F, gasoline G, and light gases/carbon L. The cracking is then described by the following three reactions

$$\begin{aligned} F &\rightarrow G \\ G &\rightarrow L \\ F &\rightarrow L. \end{aligned} \tag{1}$$

The FCC model with its modifications is described in Hovd and Skogestad (1993), and a brief summary of the FCC model equations is given in the Appendix.

Nominal steady-state optimization

For a continuous process, the overall profit of plant operation is usually given by the product values minus costs for raw material and utilities. Since the utilities are not considered in the FCC model presented above, the economic objective function comprises only product values and raw material costs and has the following form

$$\Phi = 86{,}400\left(P_{gl}F_{gl} + P_{gs}F_{gs} + P_{ugo}F_{ugo} - P_{ugo}F_{\text{feed}}\right). \tag{2}$$

The product values are given in Table 1. It is assumed that the value of unconverted gas oil is equal to the feed oil price P_{ugo} (\$/kg). The objective function is multiplied by 86,400 s/d to give the profit in the unit of \$/d.

Table 1. FCC Product Values

Component	Value
Unconverted gas oil	$P_{ugo} = \$0.088/\text{kg}$
Gasoline	$P_{gl} = \$0.14/\text{kg}$
Light gases	$P_{gs} = \$0.132/\text{kg}$

The feasible operating region of an FCC is usually limited by a number of equipment and operating constraints (Hovd and Skogestad, 1993; McFarlane et al., 1993). The process constraints are listed below:

- Maximum regenerator cyclone temperature due to the metallurgical limit of the cyclone $T_{cy} \leq 1{,}000$ K.
- Metallurgical limit of the reactor riser

$$T_{ri} \leq 1{,}000 \text{ K} \tag{3}$$

$$T_{ro} \leq 1{,}000 \text{ K}. \tag{4}$$

- Maximum air blower capacity $F_{\text{air}} \leq 60$ kg/s.
- Maximum and minimum catalyst circulation rate, 100 kg/s $\leq F_{\text{cat}} \leq 400$ kg/s.

The independent variables that will be used for control in the following are the catalyst circulation rate F_{cat} and the air flow to the regenerator F_{air} (Lee and Groves Jr., 1985; Balchen et al., 1992; Hovd and Skogestad, 1993; Alvarez-Ramirez et al., 1996). In order to analyze the economic performance of a MPC regulatory control system and the integrated control and optimization system, the nominal optimum operating point of the FCC needs to be determined. The objective function (Eq. 2) is maximized with respect to the manipulated variables F_{air} and F_{cat}, subject to the steady-state model equations and the operating constraints given above. The nominal parameter values and remaining independent variables are given in the Appendix.

The nominal optimization gives an economic optimum of $\Phi = \$36{,}905.7$/d. The corresponding input variables at the nominal optimum are $F_{\text{cat}} = 284.11$ kg/s and $F_{\text{air}} = 25.68$ kg/s. There is only one active constraint at the optimum, which is the constraint on the cyclone temperature $T_{cy} = 1{,}000$ K.

Regulatory Control of the FCC Unit

The problem of model-based control and control structure selection of the FCC processes has been addressed by several authors (Lee and Groves, Jr., 1985; Balchen et al., 1992; Hovd and Skogestad, 1993; Alvarez-Ramirez et al., 1996; Arbel et al., 1996). In the following, we shall analyze the performance of two structures previously considered by Hovd and Skogestad (1993) and Arbel et al. (1996), viz., the conventional control structure and the riser-regenerator control structure. The conventional control structure controls the temperature difference between the cyclone and the regenerator dense bed ΔT_{cy} (K) and the reactor riser outlet temperature T_{ro} (K), while the riser-regenerator control structure uses the regenerator dense bed temperature T_{reg} (K), and the riser outlet temperature T_{ro}, as controlled variables. In both structures, the manipulated variables are the catalyst circulation rate F_{cat} and the air rate to the regenerator F_{air}. Using measures of controllability such as right half plane (RHP) zeros and the frequency-dependent relative gain array (RGA), Hovd and Skogestad (1993) suggested that the riser-regenerator structure (T_{ro}, T_{reg}) is the preferred choice of control structure compared to the conventional control structure (ΔT_{cy}, T_{ro}), as the riser-regenerator control structure does not possess RHP transmission zeros within the desired bandwidth.

In the next two sections, the dynamic economics of the conventional and the riser-regenerator control structure are examined using the model predictive controller described in the first part of this article. The nonlinear process model given in the last section is linearized at the nominal steady-state optimum and discretized with a sample time of 3 min in order to obtain a discrete, linear time-invariant state-space model of the process

$$\begin{aligned} x(k+1) &= Ax(k) + B_u u(k) + B_v d(k) \\ y(k) &= Cx(k) + D_u u(k) + D_v d(k) + w(k). \end{aligned} \tag{5}$$

The disturbances d entering the process are stochastic variations in the coking characteristics of the gas oil feed, represented by the coke formation factor ψ (s^{-1}) and variations in the feed temperature T_{feed} (K). The disturbance vector $d = [\psi \; T_{\text{feed}}]^T$ is assumed to follow the linear differential equation driven by white noise $v(k)$ which is shown below

$$d(k+1) = \begin{bmatrix} 0.95 & 0 \\ 0 & 0.95 \end{bmatrix} d(k) + v(k). \tag{6}$$

The covariance of the Gaussian white noise driving the disturbances is given the following value

$$V = \begin{bmatrix} 10^{-8} & 0 \\ 0 & 1 \end{bmatrix}. \tag{7}$$

A typical profile of the disturbance variables over 12 h is shown in Figure 2.

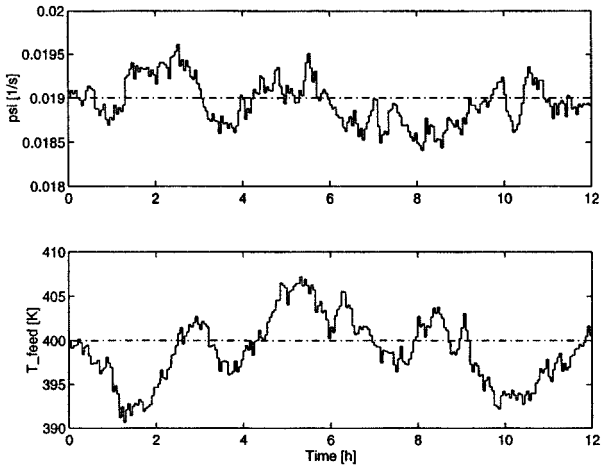

Figure 2. Stochastic disturbances in feed coking characteristics ψ and feed temperature T_{feed} over 12 hours.

(– · –) Nominal value.

Performance of the conventional control structure

The conventional control structure uses the temperature rise from the regenerator dense bed to the cyclones ΔT_{cy}, and the reactor riser outlet temperature T_{ro}, as controlled output variables, while the set of manipulated variables is $u = [F_{\text{air}}\ F_{\text{cat}}]^T$. The measurement error $w(k)$ of the controlled output variables $y = [\Delta T_{cy}\ T_{ro}]^T$ is assumed to have the following covariance matrix

$$W = \begin{bmatrix} 0.0004 & 0 \\ 0 & 0.64 \end{bmatrix}. \tag{8}$$

The dynamic economics of the conventional control structure are determined based on the unconstrained control law. The regulator was augmented with an output step disturbance vector in order to introduce an integral action into the controller. The covariance of the output variables, that is, the controlled as well as the constrained variables, is examined under closed loop. The tuning parameters, which are the objective function weighting matrices, the input prediction horizon, and the covariance of the output step disturbance vector are determined by trial and error in order to minimize the closed-loop covariance of the constrained variable T_{cy}, while, at the same time, keeping the covariance of the controlled variables ΔT_{cy} and T_{ro} as small as possible. The following tuning parameters minimize the covariance of T_{cy}

$$[Q|R|S|\Upsilon] = \left[\begin{array}{cc|cc|cc|cc} 5 & 0 & 0 & 0 & 2 & 0 & 10^{-6} & 0 \\ 0 & 3 & 0 & 0 & 0 & 0.02 & 0 & 10^{-6} \end{array}\right]. \tag{9}$$

The matrix Υ is the noise covariance matrix of the output step disturbance. The input prediction horizon was chosen to be $N = 3$. These tuning parameters gave good closed-loop covariances of the controlled and constrained output variables compared to the open-loop covariances, as can be seen in Table 2. The closed-loop covariance of T_{cy} results in a necessary backoff from the constraint due to the regulatory disturbances of $\beta_{\text{reg}} = 1.6643$ K, if feasible operation for a probability of $\alpha = 99\%$ is required. In order to obtain the dynamic economics of the conventional control structure, the necessary constraint backoff β_{reg} is introduced into the corresponding linear program (LP) as described in the first part of this article. The solution of the resulting LP gives an objective function value of $\Delta\Phi = -\$847.87$/d. This implies that the loss in economic performance due to moving away from the active cyclone temperature constraint amounts to \$847.87/d less profit, compared to the ideal case with no disturbances present.

Table 2. Covariance of Output Variables and Constraint Backoff for Conventional Control Structure

y	Open-Loop Covariance	Closed-Loop Covariance	β_{reg}
ΔT_{cy}	6.4382	0.2416	—
T_{ro}	6.3857	2.2080	—
T_{cy}	1.0048	0.5118	1.6643 K

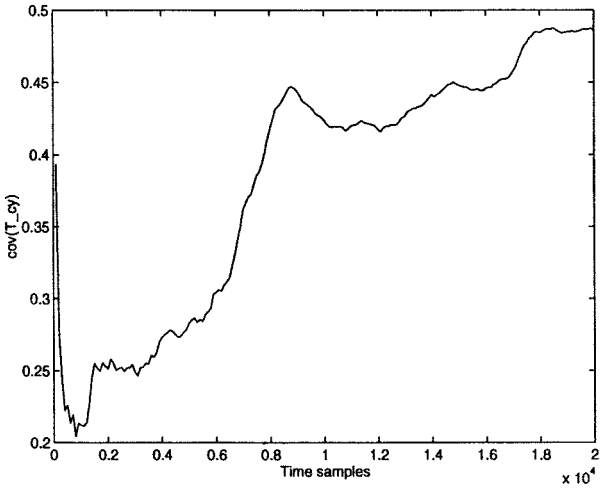

Figure 3. Convergence of covariance of T_{cy} during linear Monte Carlo simulations of conventional control structure.

The controller was applied to the nonlinear model and was simulated for 4,000 time samples, which corresponds to 200 h in order to analyze the feasibility of the backed off operating point in the presence of the regulatory disturbances. The constraint on T_{cy} was feasible for a probability of almost 100%. This might suggest that the size of the necessary backoff is overestimated by the analysis. However, Monte Carlo simulations of the closed-loop system using the linear process model showed a different reason for this behavior. The linear closed-loop system was simulated over 20,000 time samples. The simulations showed that the constraint was feasible for a probability of $\alpha = 99.94\%$, which again might indicate a conservative estimation of the size of backoff. An explanation of this behavior can be seen in Figure 3, where the covariance of the constrained variable T_{cy} as a function of time samples is shown. As can be seen, the covariance converges extremely slowly towards the value predicted by the analysis. Since the calculation of the backoff is based on the solution of the Lyapunov equations (see the first part of this article) and, therefore, considers the behavior of the system for $k \to \infty$, the analysis results can only be reproduced from linear Monte Carlo simulations when the system has converged. Thus, the seeming overestimation of the regulatory backoff for the conventional control structure stems from the extremely slow convergence of the system to the covariance of T_{cy} predicted by the analysis.

Performance of the riser-regenerator control structure

With its controlled outputs $y = [T_{\text{reg}}\ T_{ro}]^T$ and manipulated variables $u = [F_{\text{air}}\ F_{\text{cat}}]^T$, the riser-regenerator control structure is a preferred choice of control structure for the FCC process (Hovd and Skogestad, 1993). In this section, the dynamic economics of the riser-regenerator control structure are analyzed as was done in the last section for the conventional control structure. The covariance of the measurement error of the controlled output variables is assumed to take the fol-

Table 3. Covariance of Output Variables and Constraint Backoff for Riser-Regenerator Control Structure

y	Open-Loop Covariance	Closed-Loop Covariance	β_{reg}
T_{reg}	7.9251	0.4894	—
T_{ro}	6.3857	0.7417	—
T_{cy}	1.0048	0.9181	2.2290 K

lowing value

$$W = \begin{bmatrix} 1 & 0 \\ 0 & 0.64 \end{bmatrix}. \tag{10}$$

The tuning parameters of the model predictive controller were determined by trial and error in order to minimize the necessary regulatory constraint backoff. The input prediction horizon was set to $N = 3$, and the following values for the MPC objective function weighting matrices and the covariance matrix of the output step disturbance were chosen

$$[Q|R|S|\Upsilon] = \left[\begin{array}{cc|cc|cc|cc} 1 & 0 & 0 & 0 & 0 & 0 & 10^{-5} & 0 \\ 0 & 2 & 0 & 0 & 0 & 0 & 0 & 10^{-5} \end{array}\right]. \tag{11}$$

This set of tuning parameters results in good closed-loop covariances of the controlled variables T_{reg} and T_{ro}, and the constrained cyclone temperature, as can be seen in Table 3. For a required probability of feasible operation of $\alpha = 99\%$, a backoff from the cyclone temperature constraint of $\beta_{\text{reg}} = 2.2290$ K is necessary. This size of the necessary backoff corresponds to a dynamic economic performance of the riser-regenerator control structure of $\Delta\Phi = -\$1{,}135.5$/d.

The model predictive controller was applied to the nonlinear system and the feasibility of the closed-loop system in the presence of regulatory disturbances was examined. The closed-loop system was simulated for 4,000 time samples or 200 h. For this control structure, the cyclone temperature constraint was feasible for a probability of 98.62% which matches quite well the probability of feasible operation predicted by the analysis. For this control structure, the covariance of the constrained variable T_{cy} converges much faster to a value close to the covariance predicted by the analysis. This can be seen in Figure 4, where the evolution of the covariance of T_{cy} over the number of time samples during linear Monte Carlo simulations is shown. The cyclone temperature constraint was feasible for a probability of 98.82% after 20,000 time samples.

Summary

The regulatory constraint backoffs and the corresponding dynamic economic performances of two control structures of the FCC unit have been compared. Although the conventional control structure possesses a RHP transmission zero close to the origin which will limit the achievable bandwidth and the speed of response to step disturbances and set point changes, the necessary backoff is smaller and it is possible to operate the process closer to the cyclone temperature constraint for the considered stochastic disturbances compared to the riser-regenerator control structure. Since the size of the constraint backoff is associated with the loss in economic performance due to moving the operating point inside the feasible region away from the constraint, the conventional control structure would be the economically superior structure and shows better dynamic economics compared to the riser-regenerator control structure. The reason for this behavior is the fact that, for the considered set of disturbances, it is better to control ΔT_{cy} (which is equivalent to controlling the regenerator oxygen concentration) instead of T_{reg} since the disturbances in the feed coking characteristics ψ affect the coke and oxygen balances of the system.

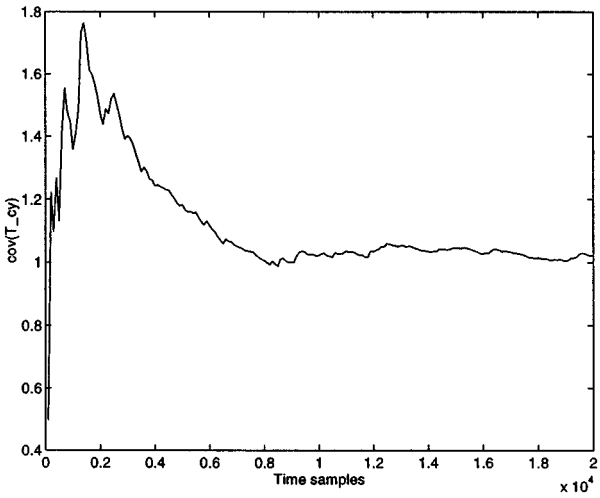

Figure 4. Convergence of covariance of T_{cy} during linear Monte Carlo simulations of riser-regenerator control structure.

On-line Optimization of the FCC Unit

In this section, the economic performance of different on-line optimizer structures is compared and an optimal structure is determined while taking into account the dynamic economics of the regulatory control structure, as analyzed in the last section. There are six uncertain process parameters which might make an on-line optimization system beneficial. The uncertain parameters together with their nominal values and the assumed standard deviation of the normally distributed uncertainty are given in Table 4. Since the plant-model mismatch for this case study is assumed to consist only in the uncertain parameter values, that is, a rig-

Table 4. Uncertain Parameters of FCC Process and Possible Model Parameter to Estimate

p	Nominal Value	σ_η
t_c	9.6 s	0.24
k_{cb}	1.9×10^{8} s^{-1}	4.75×10^{6}
λ	0.035	8.75×10^{-4}
m	80	2
k_1	9.6×10^{5} s^{-1}	2.4×10^{4}
E_g	1.126×10^{5} kJ/kmol	2815

orous model is used for optimization, the uncertain parameters given in Table 4 are also the model parameters which can be estimated during on-line optimization.

Optimizer performance with the conventional control structure

In the conventional control structure, the temperature rise from the regenerator dense bed to the cyclones ΔT_{cy} and the reactor riser outlet temperature T_{ro} are used as controlled output variables. The optimal set points at the nominal steady-state optimum are $\Delta T_{cy} = 18.428$ K and $T_{ro} = 782.745$ K. The process variables which can be measured for on-line optimization using the conventional control structure are given in Table 5 together with their expected capital and operating costs in the units of the objective function. Since the controlled output variables are kept close to a set point, they do not provide significant information about the uncertain process parameters and are not, therefore, process measurements that can be taken to estimate a set of model parameters during on-line optimization.

In order to analyze different structures of the on-line optimizer and determine the economically optimal structure, a first- and second-order perturbation model of the nonlinear steady-state model of the process is obtained at the nominal optimum. From this representation of the nonlinear problem, an analytical expression for the average deviation from optimum for a given on-line optimizer structure can be derived and a ranking of different optimizer structures in terms of their economic performance can be obtained.

After evaluating all possible online optimizer structures, the analysis suggests that the option with the smallest deviation from optimum is to estimate two parameters, namely, the residence time of the feed in the riser t_c (s) and the reaction rate constant of the gas oil cracking reaction k_1 using four of the available measurements. The selected measurements are the gasoline flow rate F_{gl} (kg/s) and the riser inlet, cyclone, and regenerator temperatures T_{ri}, T_{cy}, and T_{reg}. For this structure, the analysis predicts an average deviation from optimum of $\Theta = -\$1{,}703$/d, which is a substantial improvement against off-line optimization with an average deviation from optimum of $\Theta = -\$14{,}576$/d (see Table 6). (Off-line optimization refers to the case where no on-line parameter estimation is carried out and the process is optimized considering the *a priori* parameter uncertainty when determining the necessary constraint backoff.) Recall that the nominal optimum was $\Phi = \$36{,}905.7$/d. The size of the necessary backoff at the optimization level was determined to ensure feasible operation of the process for a probability of $\alpha = 99\%$.

Table 5. Possible Process Measurements for the Conventional Control Structure

Measurement y	σ_ϵ	Cost [\$/d]
F_{ugo}	0.002	1
T_{reg}	1	0.5
F_{gl}	0.002	1
F_{gs}	0.002	1
T_{ri}	1	0.5
T_{cy}	1	0.5

Table 6. Optimization Analysis Results for the Conventional Control Structure

	On-Line Optimization		Off-Line Optimization
	Analysis	Monte Carlo	Analysis
Θ (\$/d)	$-1{,}703$	$-1{,}694 \pm 359$	$-14{,}576$
α	99%	99.997%	99%
β_{tot}	3.2845 K	3.2845 K	25.2437 K

For this required probability, the analysis returns a backoff from the active cyclone temperature constraint of $\beta_{\text{opt}} = 1.6203$ K. Together with the necessary regulatory backoff due to fast disturbances, $\beta_{\text{reg}} = 1.6643$ K, the total size of the constraint backoff is $\beta_{\text{tot}} = 3.2845$ K (see Table 6). The results for the ten best on-line optimizer structures are given in the Appendix.

Since the analysis is based on an approximation of the nonlinear estimation and optimization problem, the analytical results are examined using nonlinear Monte Carlo simulations. The integrated system of the model predictive controller and on-line optimizer with the structure suggested by the analysis is applied to the process which is subject to both parameter uncertainty and fast disturbances as described above. After a set of measurements is taken, the selected model parameters are updated in the estimation step and new set points are calculated by the optimizer. The set points predicted by the optimizer are passed on to the regulatory control level and the process is simulated for 6 h. The deviation of the predicted from the true steady-state optimum is examined, as well as the feasibility of the cyclone temperature over that time. A total number of 2,000 runs of this on-line optimization procedure was simulated. The result is shown in Table 6. The average deviation from optimum during the nonlinear Monte Carlo simulations $\Theta = -\$1{,}694$/d matches the result predicted by the analysis quite well. Thus, the first- and second-order approximation of the problem during the analysis is justified in this case and the method gives a reliable estimation of the economic benefit of the on-line optimizer. Also, the cyclone temperature constraint was feasible for a probability of $\alpha = 99.997\%$ which more than satisfies the feasibility requirement of 99%.

In Figure 5, the profiles of the controlled variables ΔT_{cy} and T_{ro}, and the constrained variable T_{cy}, are shown for the simulation of two on-line optimizer runs. The model predictive controller is applied to the nonlinear process with the set points predicted by the on-line optimizer. The analysis of the economic performance of the integrated control and optimization system does not take the transition from one set point to another into account, so that only regulatory control at the predicted set points is shown and the transition to the new set point at $t = 6$ h is assumed to be infinitely fast. As can be seen, the controller is not able to hold the controlled variables at set points very well. This is due to the fact that the conventional control structure possesses a RHP transmission zero close to the origin, which results in a very slow closed-loop response to disturbances and long periods of a controlled variable offset from the set points. However, despite the presence of parameter uncertainty, the size of the constraint backoff is predicted quite well, since the con-

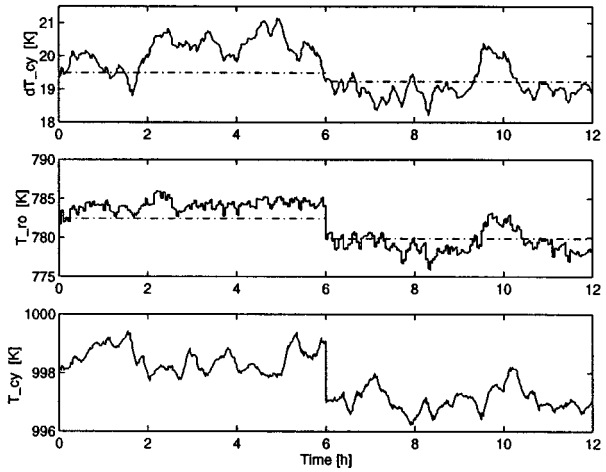

Figure 5. Output variable profiles during on-line optimization with the conventional control structure.

(–·–) Set points.

strained cyclone temperature T_{cy} is kept well below its upper bound by the controller. The corresponding profiles of the manipulated variables F_{air} and F_{cat} can be seen in Figure 6.

Optimizer performance with the riser-regenerator control structure

In this section, the optimal structure of the on-line optimizer with the riser-regenerator control structure in place is determined. The optimal set points at the nominal optimum for the riser-regenerator control structure are $T_{\text{reg}} = 981.572$ K and $T_{ro} = 782.745$ K. The process variables that can be chosen for measurement for the purpose of parameter estimation during on-line optimization are given in Table 7. Again, the controlled output variables T_{reg} and T_{ro} are not part of the possible measurements as they are kept close to a set point and do not contain significant information about

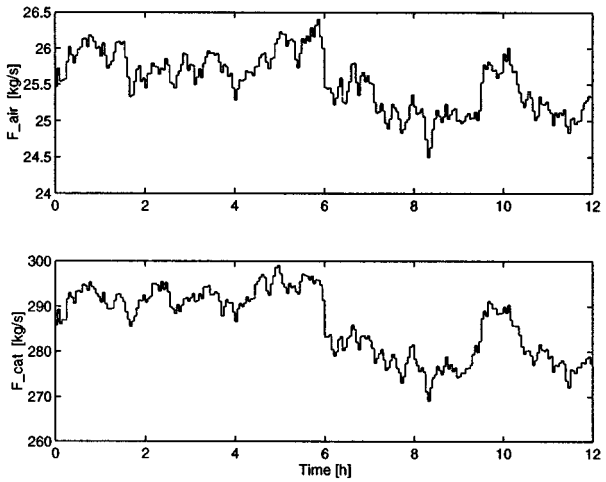

Figure 6. Input variable profiles during on-line optimization with the conventional control structure.

Table 7. Possible Process Measurements for the Riser-Regenerator Control Structure

Measurement y	σ_ϵ	Cost (\$ d)
F_{ugo}	0.002	1
ΔT_{cy}	0.02	0.5
F_{gl}	0.002	1
F_{gs}	0.002	1
T_{ri}	1	0.5
T_{cy}	1	0.5

the uncertain parameters. The set of possible measurements for on-line optimization is therefore different from that for the conventional control structure.

The average deviation from optimum is evaluated for all possible structures based on a first- and second-order perturbation model around the nominal optimum set points and parameter values. The ranking of the ten best on-line optimizer structures is given in the Appendix. The option with the smallest deviation from optimum is to estimate the residence time of the feed in the riser t_c and the rate constant of the coke combustion reaction k_{cb} (s^{-1}). The following three measurements are taken for estimating the two parameters: the flow rate of the unconverted gas oil F_{ugo} (kg/s), the temperature difference between the cyclone and regenerator dense bed ΔT_{cy}, and the flow rate of gasoline F_{gl}. The analysis predicts an average deviation from the optimum of $\Theta = -\$1{,}165$/d for this structure. Compared to an average deviation from optimum of $\Theta = -\$2{,}778$/d for off-line optimization, there exists considerable economic benefit of implementing an on-line optimization system (see Table 8), although it is significantly smaller than for the conventional control structure, where off-line optimization shows an average deviation from optimum of $\Theta = -\$14{,}576$/d (see Table 6). Feasible operation is required for a probability of $\alpha = 99\%$, which results in a backoff from the active cyclone temperature constraint of $\beta_{\text{opt}} = 0.0466$ K. With the necessary constraint backoff at the regulatory control level $\beta_{\text{reg}} = 2.2290$ K, the size of the total constraint backoff is $\beta_{\text{tot}} = 2.2756$ K (see Table 8).

The reason for the significant difference in the off-line optimization results between the conventional and the riser-regenerator control structures is the following. The energy balance in a FCC is very sensitive to parameter changes. The riser-regenerator control structure with T_{reg} and T_{ro} as controlled variables regulates the energy balance of the system. Therefore, the sensitivity of the cyclone temperature constraint with respect to changes in the uncertain parameters is greatly reduced compared to the conventional control structure, where ΔT_{cy} is a controlled variable instead of T_{reg}. Controlling ΔT_{cy} is equivalent to controlling the oxygen con-

Table 8. Optimization Analysis Results for the Riser-Regenerator Control Structure

	On-Line Optimization		Off-Line Optimization
	Analysis	Monte Carlo	Analysis
Θ (\$/d)	$-1{,}165$	$-1{,}175 \pm 25$	$-2{,}778$
α	99%	98.38%	99%
β_{tot}	2.2756 K	2.2756 K	5.3570 K

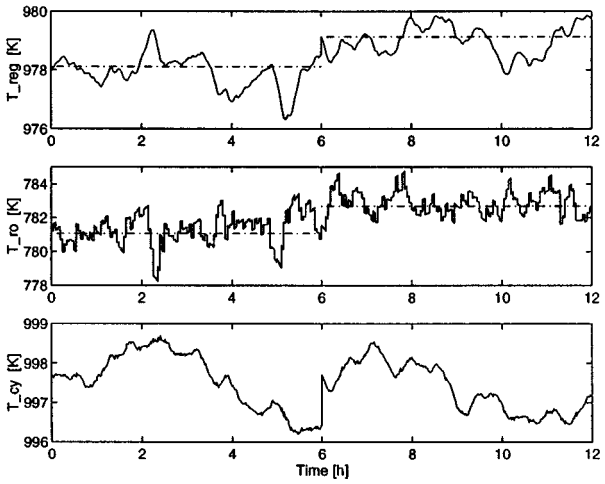

Figure 7. Output variable profiles during on-line optimization with the riser-regenerator control structure.

(– · –) Set points.

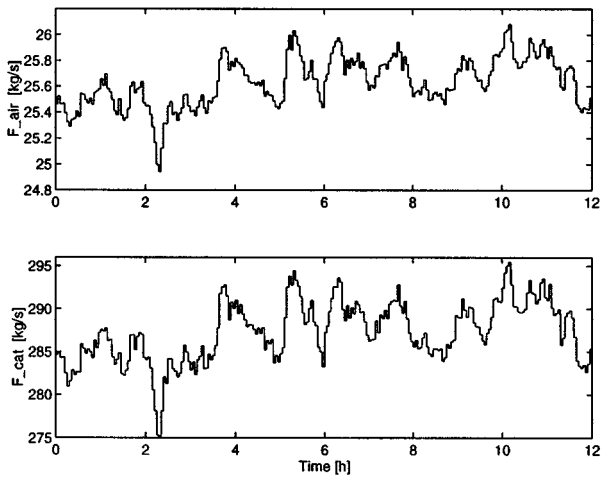

Figure 8. Input variable profiles during on-line optimization with the riser-regenerator control structure.

centration in the regenerator dense bed O_d (see Eqs. A23 and A24), which implies that the conventional control structure does not control the energy balance of the FCC. Due to the high parameter sensitivity, a very large backoff from the cyclone temperature constraint is required to accommodate the parameter uncertainty if the conventional control structure is in place.

In order to examine the analytical results of the method of the average deviation from optimum, nonlinear Monte Carlo simulations with the on-line optimizer and the model predictive controller applied to the nonlinear FCC process model were carried out. The normally distributed parameter uncertainty shown in Table 4 and the regulatory disturbances given in Eq. 6 are applied to the process. Again, 2,000 online optimization cycles are simulated and the average of the predicted from the true steady-state optimum is determined. After each on-line optimization cycle, the process is simulated for 6 h and the feasibility of the cyclone temperature constraint is examined. As can be seen in Table 8, the Monte Carlo simulations give an average deviation from the true optimum of $\Theta = -\$1{,}175$/d and the simulation result agrees quite closely within one standard deviation with the analysis result. The size of the necessary backoff from the active cyclone temperature constraint is predicted quite accurately by the analysis as the constraint is feasible for a probability of 98.38% during the simulations.

The performance of the model predictive controller applied to the nonlinear system can be seen in Figures 7 and 8. The closed-loop system is simulated for two optimization intervals and the transition from one set point to another is again neglected. Since the riser-regenerator control structure is a favorable selection of controlled and manipulated variables for the FCC process without RHP zeros, the controller can hold the controlled variables much closer to the set point in the presence of regulatory disturbances than is the case for the conventional control structure. Additionally, the constrained output variable T_{cy} is kept well below its upper bound and remains feasible for a high probability (see Figure 7). The corresponding input variable profiles are shown in Figure 8.

Summary

The economic performance of different structures of an integrated on-line optimization and regulatory control system for a FCC unit has been analyzed. The optimal structure of the on-line optimization system in terms of estimated model parameters and measured process variables has been determined for two different regulatory control structures: the conventional control structure and the riser-regenerator control structure. Although the conventional control structure shows a much better dynamic economic performance in terms of constraint backoff at the regulatory control level than the riser-regenerator control structure, the economic performance of the on-line optimizer and also the integrated optimization and regulatory control system is much better when the riser-regenerator control structure is in place and the regenerator and riser outlet temperatures are used as set points. This clearly indicates the necessity to, if possible, design the structure of the on-line optimization and regulatory control system simultaneously taking into account the economic performances of both levels in an integrated framework.

Conclusions

The theory of analyzing the economic performance of different structures of an integrated MPC regulatory control and on-line optimization system has been demonstrated on a simulated case study of a fluid-catalytic cracker (FCC). It was highlighted that the best economic performance of the on-line optimization and regulatory control system is obtained when all the structural decisions can be taken simultaneously.

Notation

A = linear state-space model matrix
B = linear state-space model matrix
c_{pair} = heat capacity of air, kJ/(kgK)

c_{pc} = heat capacity of catalyst, kJ/(kgK)
c_{pd} = heat capacity of steam, kJ/(kgK)
c_{pfl} = heat capacity of feed oil, kJ/(kgK)
C = linear state-space model matrix
C_{cat} = mass fraction of coke produced in the riser
C_{rgc} = mass fraction of coke on regenerated catalyst
C_{sc} = mass fraction of coke on spent catalyst
C_{st} = mass fraction of coke on catalyst in separator
$[COR]$ = catalyst to oil ratio
D = linear state-space model matrix
E_{cb} = activation energy for coke combustion, kJ/kmol
E_{cf} = activation energy for coke formation, kJ/kmol
E_f = activation energy for cracking of gas oil, kJ/kmol
E_g = activation energy for cracking of gasoline, kJ/kmol
f = nonlinear function or probability density function
F_{coke} = flow rate of coke deposited on catalyst, kg/s
F_{feed} = feed oil flow rate, kg/s
g = nonlinear constraint functions
k = sample time
k_i = cracking reaction rate constants, s^{-1}
K_i = cracking reaction rates, s^{-1}
m = factor for dependence of initial catalyst activity
M_{air} = molecular weight of air, kg/kmol
M_c = molecular weight of coke, kg/kmol
N = exponent for dependence of C_{cat} on C_{rgc}
O_{in} = mole fraction of oxygen in air to regenerator
p = parameters
P_{gl} = gasoline price, \$/kg
P_{gs} = price of light gases, \$/kg
Q = output weighting matrix in MPC objective function
r = set point variables
R = input weighting matrix in MPC objective function
R_{cb} = rate of coke combustion, kg/s
S = control action weighting matrix in MPC objective function
T_{air} = temperature of air to regenerator, K
T_{ri} = riser inlet temperature, K
T_{st} = separator temperature, K
V = disturbance covariance matrix
W = measurement error covariance matrix
W = holdup of catalyst in regenerator, kg
W_a = molar holdup of air in regenerator, kmol
W_{st} = holdup of catalyst in separator, kg
x = state variables
y_f = mass fraction of gas oil
y_g = mass fraction of gasoline
z = dimensionless distance along reactor riser
α = probability
α = catalyst deactivation constant, s^{-1}
δ = perturbation variable around nominal optimum
ΔH_{CO} = heat of CO combustion, kJ/kmol
ΔH_{CO_2} = heat of CO_2 combustion, kJ/kmol
ΔH_f = heat of cracking, kJ/kg
ϵ = normally distributed measurement error
η = normally distributed parameter uncertainty
θ = dimensionless temperature in reactor riser
Θ = average deviation from optimum
λ = mass ratio of dispersion steam to feed oil
σ = standard deviation
σ = molar ratio of CO_2 to CO
ϕ = deactivation of catalyst
Φ = economic objective function
Ψ = constraint covariance matrix

Literature Cited

Alvarez-Ramirez, J., R. Aguilar, and F. Lopez-Isunza, "Robust Regulation of Temperature in Reactor-Regenerator Fluid Catalytic Cracking Units," *Ind. Eng. Chem. Res.*, **35**, 1652 (1996).

Arbel, A., Z. Huang, I. H. Rinard, R. Shinnar, and A. V. Sapre, "Dynamics and Control of Fluidized Catalytic Crackers. 1. Modeling of the Current Generation of FCCs," *Ind. Eng. Chem. Res.*, **34**, 1228 (1995).

Arbel, A., I. H. Rinard, and R. Shinnar, "Dynamics and Control of Fluidized Catalytic Crackers. 3. Designing the Control System: Choice of Manipulated and Measured Variables for Partial Control," *Ind. Eng. Chem. Res.*, **35**, 2215 (1996).

Balchen, J. G., D. Ljungquist, and S. Strand, "State-Space Predictive Control," *Chem. Eng. Sci.*, **47**, 787 (1992).

Cutler, C. R., and R. T. Perry, "Real Time Optimization with Multivariable Control is Required to Maximize Profits," *Comp. Chem. Eng.*, **7**, 663 (1983).

de Hennin, S. R., J. D. Perkins, and G. W. Barton, "Structural Decisions in On-Line Optimization," *Proc. of Int. Conf. on Process Systems Eng. PSE '94*, 297 (1994).

Errazu, A. F., H. I. DeLasa, and F. Sarti, "A Fluidized Bed Catalytic Cracking Regenerator Model. Grid Effects," *Can. J. Chem. Eng.*, **57**, 191 (1979).

Hovd, M., and S. Skogestad, "Procedure for Regulatory Control Structure Selection with Application to the FCC Process," *AIChE J.*, **39**, 1938 (1993).

Jacob, S. M., B. Gross, S. E. Voltz, and V. W. Weekman, Jr., "A Lumping and Reaction Scheme for Catalytic Cracking," *AIChE J.*, **22**, 701 (1976).

Lee, E., and F. R. Groves, Jr., "Mathematical Models of the Fluidized Bed Catalytic Cracking Plant," *Trans. Soc. Comp. Sim.*, **2**, 219 (1985).

Lee, L.-S., Y.-W. Chen, and T.-N. Huang, "Four-Lump Kinetic Model for Fluid Catalytic Cracking Process," *Can. J. Chem. Eng.*, **67**, 615 (1989).

Loeblein, C., and J. D. Perkins, "Economic Analysis of Different Structures of On-Line Process Optimization Systems," *Comp. Chem. Eng.*, **20**, S551 (1996).

McFarlane, R. C., R. C. Reineman, J. F. Bartee, and C. Georgakis, "Dynamic Simulator for a Model IV Fluid Catalytic Cracking Unit," *Comp. Chem. Eng.*, **17**, 275 (1993).

Qin, S. J., and T. A. Badgwell, "An Overview of Industrial Model Predictive Control Technology," *Proc. of the 5th Conference on Chem. Process Control CPC-V*, Tahoe City (1996).

Appendix: Process Model, Parameter Values and Results of the FCC Case Study

FCC model equations

The reactor riser is modeled as a quasi steady-state plug-flow reactor where the reactions given in Eq. 1 are taking place. The gas oil cracking reactions are described by second-order kinetics while the overcracking reaction from gasoline to the light gases is described by first-order kinetics:

- Material balance for gas oil F

$$\frac{dy_f}{dz} = -K_1 y_f^2 [COR] \phi t_c, \quad y_f(z=0) = 1, \qquad \text{(A1)}$$

where K_1 is the reaction rate of the total cracking of gas oil

$$K_1 = k_1 \exp\left(\frac{-E_f}{RT_{ri}(1+\theta)}\right). \qquad \text{(A2)}$$

- Material balance for gasoline G

$$\frac{dy_g}{dz} = \left(K_2 y_f^2 - K_3 y_g\right)[COR]\phi t_c, \quad y_g(z=0) = 0 \qquad \text{(A3)}$$

where K_2 is the reaction rate of the gasoline production and K_3 is the rate of the overcracking reaction:

$$K_2 = k_2 \exp\left(\frac{-E_f}{RT_{ri}(1+\theta)}\right) \qquad \text{(A4)}$$

$$K_3 = k_3 \exp\left(\frac{-E_g}{RT_{ri}(1+\theta)}\right) \qquad \text{(A5)}$$

The catalyst to oil ratio is given by $[COR] = F_{cat}/F_{feed}$ and t_c is the residence time of the reaction mixture in the riser. The variable z is the dimensionless distance along the riser, where $z = 0$ denotes the bottom and $z = 1$ the top of the riser.

- The deactivation of catalyst ϕ due to coke deposition is given by

$$\phi = (1 - mC_{rgc}) \exp(-\alpha t_c [COR] z). \quad \text{(A6)}$$

- The amount of coke produced is estimated using the following correlation

$$C_{cat} = \psi \sqrt{\frac{t_c}{C_{rgc}^N} \exp\left(\frac{-E_{cf}}{RT_{ro}}\right)}. \quad \text{(A7)}$$

The amount of coke on the catalyst leaving the riser is thus

$$C_{sc} = C_{rgc} + C_{cat}. \quad \text{(A8)}$$

A simple material balance gives the amount of coke produced during the cracking reactions, while the product flows (kg/s) of unconverted gas oil F_{ugo}, gasoline F_{gl}, and light gases F_{gs} are given by the material balances for gas oil and gasoline

$$F_{coke} = F_{cat}(C_{sc} - C_{rgc}) \quad \text{(A9)}$$

$$F_{ugo} = y_f(1) F_{feed} \quad \text{(A10)}$$

$$F_{gl} = y_g(1) F_{feed} \quad \text{(A11)}$$

$$F_{gs} = (1 - y_f(1) - y_g(1)) F_{feed} - F_{coke}. \quad \text{(A12)}$$

- The quasi steady-state energy balance along the riser together with the riser entrance temperature $T_{ri} = T(z = 0)$ is given by

$$\frac{d\theta}{dz} = \frac{\Delta H_f F_{feed}}{T_{ri}(F_{cat} c_{pc} + F_{feed} c_{pfl} + \lambda F_{feed} c_{pd})} \frac{dy_f}{dz} \quad \text{(A13)}$$

$$\theta(z) = \frac{T(z) - T_{ri}}{T_{ri}}, \quad \theta(z = 0) = 0, \quad T_{ro} = T(z = 1) \quad \text{(A14)}$$

$$T_{ri} = \frac{(F_{feed} c_{pfl} + \lambda F_{feed} c_{pd}) T_{feed} + F_{cat} c_{pc} T_{reg}}{F_{feed} c_{pfl} + \lambda F_{feed} c_{pd} + F_{cat} c_{pc}}. \quad \text{(A15)}$$

The regenerator model consists of the balance equations for coke, oxygen, and energy.

- Material balance for coke on regenerated catalyst

$$W \frac{dC_{rgc}}{dt} = F_{cat}(C_{st} - C_{rgc}) - R_{cb}. \quad \text{(A16)}$$

The rate of coke combustion is given by the following relationship

$$R_{cb} = k_{cb} \exp\left(-\frac{E_{cb}}{RT_{reg}}\right) O_d C_{rgc} W. \quad \text{(A17)}$$

- Oxygen balance in the regenerator dense bed

$$W_a \frac{dO_d}{dt} = \frac{F_{air}}{M_{air}}(O_{in} - O_d) - \frac{1 + 1.5\sigma}{1 + \sigma} \frac{R_{cb}}{M_c}. \quad \text{(A18)}$$

The variable σ denotes the ratio of CO_2 to CO produced during the coke combustion reactions. In the considered operating region, it is assumed to be linearly dependent on the regenerator temperature

$$\sigma = 1.1 + 0.0061(T_{reg} - 873). \quad \text{(A19)}$$

- The regenerator energy balance is given by the following relationship

$$Wc_{pc} \frac{dT_{reg}}{dt} = F_{cat} c_{pc} T_{st} + F_{air} c_{pair} T_{air} - (F_{cat} c_{pc} + F_{air} c_{pair}) T_{reg} - \left(\Delta H_{CO} + \frac{\sigma}{1 + \sigma} \Delta H_{CO_2}\right) \frac{R_{cb}}{M_c}. \quad \text{(A20)}$$

The heats of reaction, ΔH_{CO} and ΔH_{CO_2}, are given by the following empirical relationships

$$\Delta H_{CO} = -361{,}465.3 + 16.23 T_{reg} - 31.92 \times 10^{-4} T_{reg}^2 + 18.67 \times 10^{-7} T_{reg}^3 + 1{,}275{,}299.0/T_{reg} \quad \text{(A21)}$$

$$\Delta H_{CO_2} = -284{,}375.0 - 1.653 T_{reg} + 29.51 \times 10^{-4} T_{reg}^2 + 425.588.2/T_{reg}. \quad \text{(A22)}$$

- The increase in temperature of the cyclones compared to the regenerator dense bed is assumed to be linearly dependent on the oxygen concentration in the regenerator dense bed

$$T_{cy} = T_{reg} + 5{,}555 O_d. \quad \text{(A23)}$$

The temperature rise from the regenerator dense bed to the cyclones is then given by

$$\Delta T_{cy} = T_{cy} - T_{reg}. \quad \text{(A24)}$$

The separator is modeled simply as an ideal mixing tank with coke and energy balances, which introduces a lag between the riser outlet and the catalyst return to the regenerator

$$W_{st} \frac{dC_{st}}{dt} = F_{cat}(C_{sc} - C_{st}) \quad \text{(A25)}$$

$$W_{st} c_{pc} \frac{dT_{st}}{dt} = F_{cat} c_{pc}(T_{ro} - T_{st}). \quad \text{(A26)}$$

The model describes the partial combustion mode of the FCC. The independent variables and nominal parameter values of the FCC model are given below. The complete combustion

mode can be described using the same model with a few modifications which are outlined by Hovd and Skogestad (1993).

Parameter values of the FCC model

$c_{pfl} = 3.1335$ kJ/kg·K
$c_{pc} = 1.005$ kJ/kg·K
$c_{pd} = 1.9$ kJ/kg·K
$c_{\text{pair}} = 1.05$ kJ/kg·K
$\lambda = 0.035$
$k_1 = 9.6\times10^5$ s^{-1}
$k_2 = 4.224\times10^5$ s^{-1}
$k_3 = 7.2\times10^5$ s^{-1}
$t_c = 9.6$ s
$E_f = 1.015\times10^5$ kJ/kmol
$E_g = 1.126\times10^5$ kJ/kmol
$R = 8.31451$ kJ/kmol·K
$\alpha = 0.12$ s^{-1}
$\Delta H_f = 506.2$ kJ/kg
$m = 80$
$E_{cf} = 41{,}790$ kJ/kmol
$M_{\text{air}} = 28.8544$ kg/kmol
$M_c = 14$ kg/kmol
$k_{cb} = 1.9\times10^8$ s^{-1}
$\psi = 0.019$ s^{-1}
$N = 0.4$
$O_{\text{in}} = 0.2136$

Independent variables of the FCC model

$F_{\text{feed}} = 40.63$ kg/s
$T_{\text{feed}} = 400$ K
$T_{\text{air}} = 320$ K
$W = 175{,}738$ kg
$W_a = 20$ kmol
$W_{st} = 17{,}500$ kg
$E_{cb} = 157{,}884.23$ kJ/kmol

Optimal FCC on-line optimizer structures

In this section, the rankings of the ten best on-line optimizer structures for both the conventional and the riser-regenerator control structure are given. The on-line optimizer structures together with the necessary constraint backoff, β_{tot}, and the average deviation from optimum, Θ, are shown in Tables A1 and A2.

Table A1. Ten Best FCC On-Line Optimizer Structures for the Conventional Control Structure

Measurements	Estimated Parameters	β_{tot} (K)	Θ ($/d)
T_{reg}, F_{gl}, T_{ri}, T_{cy}	t_c, k_1	3.2845	−1,703.04
T_{reg}, T_{ri}, T_{cy}	t_c	3.2987	−1,710.07
T_{reg}, F_{gl}, T_{ri}, T_{cy}	t_c, E_g	3.2987	−1,711.01
T_{reg}, F_{gs}, T_{ri}, T_{cy}	t_c, E_g	3.2987	−1,711.09
T_{reg}, F_{gs}, T_{ri}, T_{cy}	t_c, k_1	3.3007	−1,712.20
T_{reg}, T_{ri}, T_{cy}	k_{cb}	3.2954	−1,713.11
T_{reg}, F_{gl}, T_{ri}, T_{cy}	k_{cb}, E_g	3.2954	−1,713.87
F_{ugo}, T_{reg}, F_{gs}, T_{ri}, T_{cy}	t_c, λ, k_1	3.3046	−1,714.00
T_{reg}, F_{gs}, T_{ri}, T_{cy}	k_{cb}, E_g	3.2954	−1,714.21
F_{ugo}, T_{reg}, T_{ri}, T_{cy}	t_c, λ	3.3063	−1,714.31

Table A2. Ten Best FCC On-Line Optimizer Structures for the Riser-Regenerator Control Structure

Measurements	Estimated Parameters	β_{tot} (K)	Θ ($/d)
F_{ugo}, ΔT_{cy}, F_{gl}	t_c, k_{cb}	2.2756	−1,164.99
F_{ugo}, ΔT_{cy}, F_{gl}, T_{cy}	t_c, k_{cb}	2.2756	−1,165.49
F_{ugo}, ΔT_{cy}, F_{gl}, T_{ri}	t_c, k_{cb}	2.2756	−1,165.49
F_{ugo}, ΔT_{cy}, F_{gs}	t_c, λ, k_1	2.2755	−1,165.52
F_{ugo}, ΔT_{cy}, F_{gl}, T_{ri}, T_{cy}	t_c, k_{cb}	2.2756	−1,165.99
F_{ugo}, ΔT_{cy}, F_{gs}, T_{cy}	t_c, λ, k_1	2.2755	−1,166.01
F_{ugo}, ΔT_{cy}, F_{gs}, T_{ri}	t_c, λ, k_1	2.2755	−1,166.02
F_{ugo}, ΔT_{cy}, F_{gl}	t_c, k_{cb}, k_1	2.2755	−1,166.02
F_{ugo}, ΔT_{cy}, F_{gs}	t_c, k_{cb}, k_1	2.2755	−1,166.02
ΔT_{cy}, F_{gl}, F_{gs}	t_c,k_{cb}, k_1	2.2755	−1,166.02

Manuscript received Feb. 23, 1998, and revision received Jan. 12, 1999.